Journal of Hydrology 498 (2013) 274–286

Contents lists available at SciVerse ScienceDirect

Journal of Hydrology

journal homepage: www.elsevier.com/locate/jhydrol

Hydrochemical, mineralogical and isotopic investigation of arsenic distribution and mobilization in the Guandu wetland of Taiwan

Yu-Hsuan Kao [a], Sheng-Wei Wang [b], Sanjoy Kumar Maji [a], Chen-Wuing Liu [a,*], Pei-Ling Wang [c], Fi-John Chang [a], Chung-Min Liao [a]

[a] Department of Bioenvironmental Systems Engineering, National Taiwan University, Taipei 106, Taiwan, ROC
[b] Sinotech Environmental Technology, Taipei 105, Taiwan, ROC
[c] Institute of Oceanography, National Taiwan University, Taipei 106, Taiwan, ROC

ARTICLE INFO

Article history:
Received 20 November 2012
Received in revised form 14 April 2013
Accepted 7 June 2013
Available online 20 June 2013
This manuscript was handled by Laurent Charlet, Editor-in-Chief, with the assistance of Jiin-Shuh Jean, Associate Editor

Keywords:
Arsenic
Wetland ecosystem
Mineralogical compositions
Stable sulfur isotope
Redox cycling

SUMMARY

This study explores the distribution and mobilization of As in the ecosystem of the Guandu wetlands, Taiwan. The chemical parameters, chemical sequential extraction, mineralogical compositions, and sulfur isotopic compositions (i.e., $\delta^{34}S_{[SO4]}$ and $\delta^{18}S_{[SO4]}$) of porewater and two sediment core samples (S2 and S5, locate in the inner and outer sites of the Guandu wetland) were analyzed to characterize As spatial distribution. The crucial mechanisms of the biogeochemical processes that control As mobility in wetland ecosystems were inferred. Based on factor analysis and cluster analysis, the vertical distributions of the redox zones in S2 and S5 were classified as oxidizing, transitional, and reducing zones, respectively. The mineralogical characteristics showed that adsorption and desorption are the major processes which control As retention in the surface sediment under cyclic aerobic/anaerobic conditions. Aqueous As and Fe were restrained because of oxidation, whereas aqueous Fe precipitated as amorphous metal oxides (i.e., FeO, FeOOH, and Fe_2O_3). Subsequently, aqueous As was adsorbed onto the surfaces of Fe(hydr)oxides, resulting in a high solid As content in the oxidizing zone. The high aqueous As content in the boundary of the transitional and reducing zones was caused by the reductive dissolution of highly dissolved Fe compounds through the microbial respiration of organic matter (OM). In the reducing zone, As^{3+} can be constrained by the formation of FeS_2 in sediment during bacterial sulfate reduction that is governed by the relative enrichment of the $\delta^{34}S_{[SO4]}$ and $\delta^{18}S_{[SO4]}$ values. Sulfur disproportionation and the redox of elemental sulfur (S^0) are additional reaction paths that cause As cycling. Arsenic mobility in the Guandu wetland is primarily caused by the reductive dissolution of As-containing Fe-oxyhydroxides and the redox cycling of sulfate/sulfide, accompanied by the respiration of OM.

© 2013 Elsevier B.V. All rights reserved.

1. Introduction

Wetlands can accumulate nutrients and anthropogenic substances in downstream eutrophication ecosystems. Solid Fe and Mn oxyhydroxides act as a sink for many trace elements in reducing environments (Carroll et al., 1998; Lytle et al., 1998). Arsenic in organic-rich wetlands can limit transformation and mobilization (La Force et al., 2000; Bauer et al., 2008; Du Laing et al., 2009). The redox cycling of As in wetland systems is largely determined by (1) in situ redox conditions, (2) the dissolution–precipitation of minerals with arsenic as a constituent ion, and (3) sorption–desorption (La Force et al., 2000, Mandal et al., 2009, 2012). The redox states of solid As stability complexes (Goldberg, 2002) and co-precipitates (Waychunas et al., 1993) are thermodynamically controlled. The geochemical characteristics of As mobility are strongly influenced by iron, sulfur, and carbon redox processes, which may be primarily governed by the metabolic activity of bacteria (Pierce and Moore, 1982; Wilkin and Ford, 2006; Mukherjee and Fryar, 2008). A strong correlation of aqueous As^{3+} and Fe^{2+} concentrations are observed in low-level redox potential. For example, the binding of As and Fe in the same solid phase pools has been found in strongly minerotrophic and Fe-rich fen. Redox-related processes in aquifers/wetlands are largely controlled by the reduction of FeOOH in the presence of organic matter (OM) during bacteria respiration, serving as electron donors (McArthur et al., 2001, 2004; Harvey et al., 2002; Zheng et al., 2004; Cancès et al., 2005; Hossain et al., 2012).

In oxidizing conditions, low As mobility is caused by the formation of As^{5+} and its subsequent adsorption of metal oxides. Arsenic anions can sorb or bind using carbonates (Bauer et al., 2008; Rothwell et al., 2009) and silicates (Goldberg, 2002), but Al, Mn, and especially Fe oxides are the most crucial As sorbents in oxic conditions because of their large reactive surface areas (Smedley

* Corresponding author. Tel.: +886 2 2362 6480; fax: +886 2 2363 9557.
E-mail address: lcw@gwater.agec.ntu.edu.tw (C.-W. Liu).

0022-1694/$ - see front matter © 2013 Elsevier B.V. All rights reserved.
http://dx.doi.org/10.1016/j.jhydrol.2013.06.009

and Kinniburgh, 2002; Wang and Mulligan, 2006, 2008). The oxygenation of Fe^{2+} containing water to induce iron precipitation is used for sorbing and removing of As during As-contaminated water treatment processes (Jessen et al., 2005). Analytical methods have been used to accurately determine As oxidation states and local coordination environments in various solid phases and its possible presence as a surface-bound or adsorbed species. The chemical sequential extraction method is frequently used to determine operationally defined fractions. Spectroscopic methods, including X-ray techniques and vibrational spectroscopy, entail measuring the amount of energy absorbed or emitted by a system in response to an external perturbation in the form of electromagnetic radiation. The local coordination environments of As^{3+} and As^{5+} sorbed to natural or synthetic iron oxides of varying crystallinity have been widely investigated and compared with X-ray absorption near-edge structure (XANES) spectroscopic techniques (Manning et al., 2002; Sherman and Randall, 2003). The varying affinities of As^{3+} and As^{5+} can affect the extent of their sorption in sediment. The various capacities for As sorption onto sediment may affect As' concentration in water. In anoxic sediments, dissolved sulfates are terminal electron acceptors and are used by sulfate-reducing bacteria (SRB) during the heterotrophic respiration of OM (Jørgensen, 1982). A crucial pathway regarding trace metal behavior in sediments is the reaction of dissolved sulfide with ferrous iron to precipitate Fe sulfides, which may be responsible for metal uptake through sorption and/or co-precipitation (Xia et al., 1998; Wang and Mulligan, 2008; Langner et al., 2012). Fe disulfide and pyrite are important carriers of As (Dellwig et al., 2002; Bostick and Fendorf, 2003). Most metal sulfides provide a potential sink for As in anoxic sediments (Dellwig et al., 2002). Under sulfate-reducing conditions, As adsorption on the surfaces of metal sulfides and/or co-precipitation is the most crucial uptake process (Farquhar et al., 2002; Wolthers et al., 2005). Numerous studies have indicated that isotopic techniques are useful for understanding the influence of sulfur cycling geochemical environmental conditions on As mobility (Lipfert et al., 2007; Mukherjee and Fryar, 2008; Kao et al., 2011).

High As concentrations occur naturally in geothermal areas because of volcanic activity, resulting in pollution in groundwater, geothermal spring water, and downstream of the Guandu wetland ecosystem. However, the distribution and mobilization of As in the wetland ecosystem are not well understood. This study examines the geochemical processes of As in the Guandu wetland. We investigate the geochemical characteristics and processes of As in wetlands using advanced technologies, including chemical analyses, stable isotopic analyses, and spectroscopic methods. Finally, a conceptual model for the biogeochemical processes of aqueous and solid As cycling in the Guandu wetland is proposed.

2. Materials and methods

2.1. Study area

The Guandu wetland is located in the northern part of the Guandu Plain in Taipei, Taiwan, which is the downstream of the Beitou geothermal spring (Fig. 1). In the 1960s, many geothermal fields of Beitou have been developed to generate energy from the steam and hot water reservoirs of Tatun Volcano Group. Large scale andesitic volcanic eruptions took place in north and northeast offshore islands of Taiwan during the Pleistocene. Both andesitic lavas and andesitic pyroclastics are presented. Acidic hot spring water has high arsenic, sulfate and lead concentrations. Previous studies revealed that As concentration in the hot spring water was up to 4.32 mg/L and overly exceeded the drinking water guideline of WHO, 0.01 mg/L (Wang, 2005; Chiang et al., 2010). The As-rich spring water flows to Huang Gang Creek, discharging a high-As flux to the Guandu Plain. Long-term irrigation with high As concentration water has caused the high average As contents of 145 and 143 mg/kg in the upper (0–15 cm) and lower (15–30 cm) soils, respectively, in the Guandu Plain, markedly exceeds the soil contamination standard of 60 mg/kg (Chiang et al., 2010). Arsenic-rich spring water flows to the downstream wetland, and may alter aqueous and solid-phase compositions. As contents were as high as 1–5 g/kg in the coarse fraction (>0.25 mm) soil samples (Wu, 2008).

The Guandu wetland is near to the mouth of the Keelung and Tanshui Rivers, it has a semi-diurnal tidal regime with a tidal amplitude of approximately 1–2 m; and although it is only 10 km away from the Tanshui River estuary, the wetland area is widely affected by tidal fluctuations. Tidal seawater, which can intrude into the upper estuary approximately 25 km away from the river mouth, mixes with the river water during high tide, but only partially mixes during low tide (Liu et al., 2001). Seawater mixing with fresh water may provide excessive amount of competition ions such as Cl^- and SO_4^{2-} which can theoretically function as HCO_3^- and PO_4^{3-}. The effect of ionic competition against the adsorption site of As onto the surface of metal oxides is also assessed (Kim et al., 2000; Appelo et al., 2002). Hence, the variations of salinity, pH, and redox conditions may potentially affect the As releases and the retention reactions in wetland system.

2.2. Water, soil and plant sampling

Porewater and sediment samples of core were collected at the inner (S2 = 70 cm) and outer sites (S5 = 85 cm) of Guandu wetland in April, 2010 (Fig. 1). Porewater samples with an interval of 5 cm were extracted using a Rhizon sampler (microporous polymer, <0.2 μm pore size). The sediment samples with an interval of 5 cm were air-dried to facilitate the analyzing of chemical compounds. Porewater and sediment samples in both cores with an interval of 10 cm were extracted for isotopic analyses. Water samples were stored in polyethylene containers, maintained at 4 °C, and sent to the laboratory within 24 h. Sediment samples were stored in N_2-purged plastic bags, dried at room temperature, and homogenized using 100-mesh sieves in an anaerobic glove box. The split samples were removed from the glove box and allowed to oxidize in an oven at 50 °C for 72 h. Chemical compositions, speciation of As and Fe, chemical sequential extraction, and isotopic compositions in aqueous phase and/or solid phase were analyzed.

2.3. Chemical compounds of water and soil analysis

The dissolved oxygen (DO), redox potential (Eh), electrical conductivity (EC) and pH of the porewater samples were measured at S2 and S5. Porewater samples were filtered through 0.45-μm glass fiber papers. Unacidified parameters (NO_3^-, Cl^-, and SO_4^{2-}) and acidified parameters (NH_4^+, Ca^{2+}, Mg^{2+}, Na^+, K^+, Fe and Mn) were used to measured by ion chromatography (by, DIONEX ICS-900). Bicarbonate was determined by acid titration. Porewater samples for metals and other ionic concentrations measurements were with 0.45 μm nylon filters and acidified with various acids for specific analysis (APHA, 1998). Ferrous (Fe^{2+}) concentrations of the samples were measured colorimetrically using the ferrozine method (Lovley and Phillips, 1987). Analytical method of As^{3+}, As^{5+}, MMA, and DMA followed closely from our previous study (Huang et al., 2003). The variances of duplicate measurements were less than 10%; recoveries of check and spike samples were between 85% and 115%, respectively. Moreover, chemical sequential extraction was conducted for the determination of As concentrations in the various mineral phases (Bauer et al., 2008). The extraction

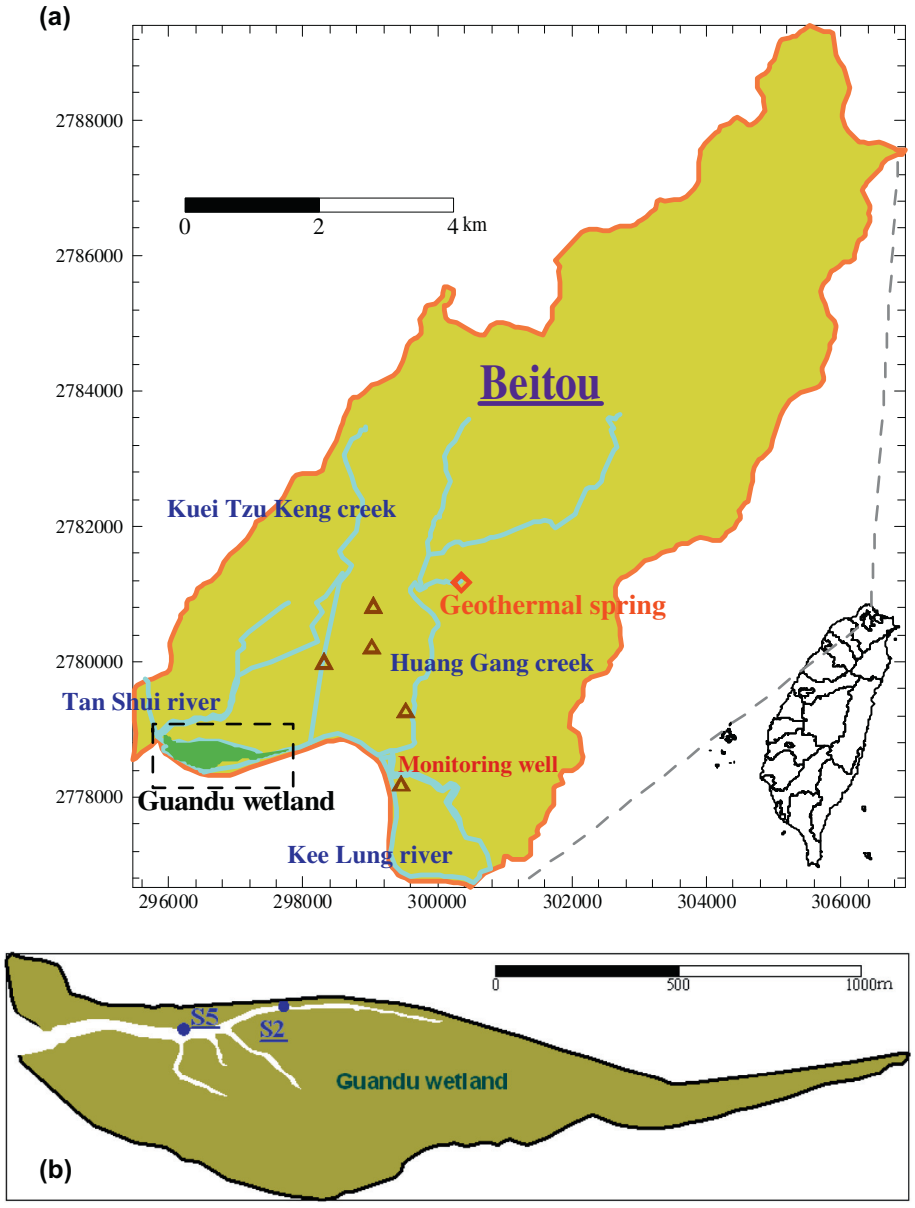

Fig. 1. (a) Study area and (b) core sampling locations of Guandu wetland.

consisted of four steps, including (1) exchangeable, (2) amorphous metal oxides and carbonate, (3) crystalline metal oxides, and (4) aluminosilicates and sulfides. Detailed experimental and analytical procedures were described in Bauer et al. (2008).

Sediment samples were air-dried, digested in aqua regia, and filtered to determine the trace metals concentration like total As, Fe, Mn, using ICP-MS. Sulfate and total organic carbon contents were analyzed by turbidimetric method and Walkley–Black method, respectively.

2.4. Sulfide and sulfur isotope analyses

Porewater samples were filtered and acidified with 1 M HCl to maintain the solution pH < 2; 10% $BaCl_2$ was then added to the samples to produce $BaSO_4$ precipitation. The samples were then filtered and dried (Yanagisawa and Sakai, 1983). Precipitated $BaSO_4$ were recovered by centrifugation, carefully washed in double distilled water and dried prior to isotope analysis. The $\delta^{34}S_{[SO4]}$ and $\delta^{18}S_{[SO4]}$ were analyzed in the isotope laboratory of the University of Arizona using a continuous-flow gas-ratio mass spectrometer (Thermo Scientific Delta PlusXL). Sulfur isotope analysis of the sulfide minerals ($\delta^{34}S_{[FeS_2]}$) was performed via reduced inorganic sulfur by diffusion method (Hsieh and Shieh, 1997). Before analyzing the sulfur isotope from the sediment samples, acid-volatile sulfide (AVS; FeS), chrome-reducible sulfide (CRS; FeS_2–S) and elemental sulfur (ES; S^0) were determined using chemical sequential extraction methods. Briefly, AVS, CRS and ES were separated sequentially by 6 M HCl (18 h), acidic Cr(II) (48 h) and N, N-dimethylformamide (DMF) (24 h), respectively, under pure N_2 gas, at ambient temperature (25 ± 3 °C). The liberated H_2S was then passively trapped in an alkaline Zn solution which was in a small beaker containing a 15 mL 3% alkaline zinc (Zn) acetate solution that was placed in a bottle. However, the undetected AVS and ES in sediment samples of S2 and S5 may be caused by the unstable formation and/or lack of mackinawite (FeS) and elemental sulfur in natural environment. The $\delta^{34}S_{[FeS_2]}$ was analyzed using ZnS powder in the isotope

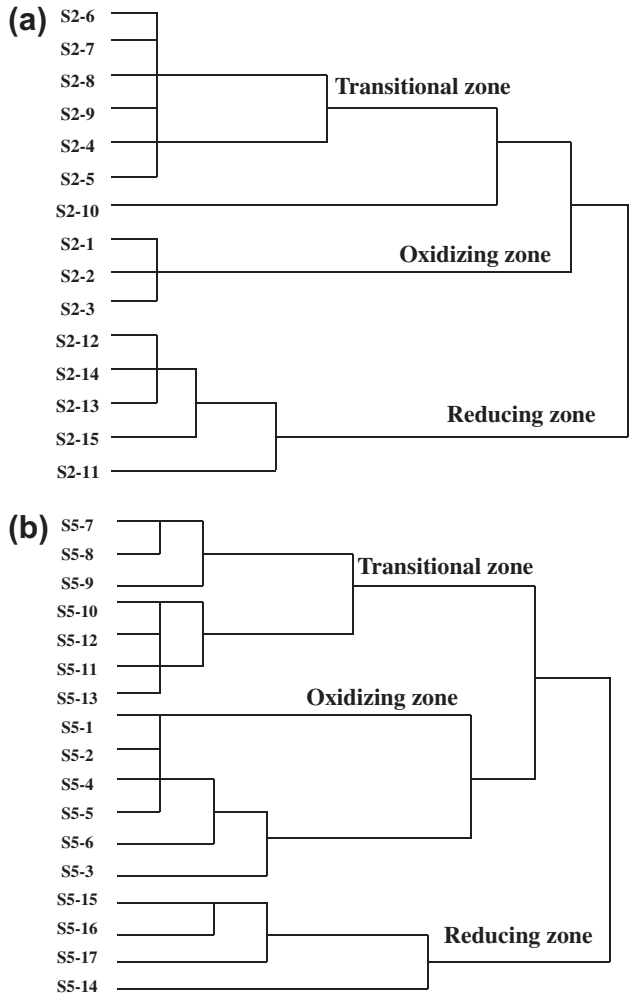

Fig. 2. Dendrograms of all porewater of (a) S2 and (b) S5 by CA in the Guandu wetland.

laboratory of the University of Arizona by the Thermo Scientific Delta PlusXL.

2.5. Mineralogical characterization

To characterize the surface chemical properties and compositions of the core samples, XPS (X-ray photoelectron spectroscopy) and SEM–EDS (Scanning electron microscope and energy dispersive spectrometer) were introduced. Feature of main As-bearing phase (such as probable ferrihydrites with various Fe/As molar ratios) exits in which As is present as surface-sorbed and/or incorporated species is need to explore. Chemical characterizations of well-screened core samples in both cores of S2 and S5 are identified by the high resolution X-ray photoelectron spectroscopy (HR-XPS; ULVAC-PHI PHI Quantera SXM) and scanning electron microscope (SEM; Hitachi S-3000N). Both XPS and SEM are of surface chemical analysis techniques and can be used to analyze the surface chemistry of materials. XPS provides information on the elemental compositions, empirical formulas, chemical states and electronic states of the elements that exist within the surfaces or reaction layers of minerals and grains (Frau et al., 2005). SEM is designed for direct studying of the surfaces of solid objects, and has great depth of field yielding three-dimensional characteristics appearance useful for understanding the surface structure of a mineral (Hou et al., 2006). The X-ray absorption near-edge structure (XANES) spectra were used to determine As speciation in the sediment samples. X-ray absorption spectra (XAS) at the As K-edge (11,867 eV) were collected at the Wiggler 20 beamline BL-17C at the NSRRC. Sample spectra regarding the As Kα edge of 11,867 eV were collected from −50 to +100 eV, and then compared to XANES spectra with the selected reference standards, including arsenate ($Na_2HAsO_4{\cdot}7H_2O$) and arsenite ($NaAsO_2$). Several scans of each sample were processed and averaged to improve the data quality of XAS spectra. The Athena program was employed for standard background subtraction and edge-height normalization using the AUTOBK algorithm (Ravel and Newville, 2005). Core samples S2 (5, 25 and 65 cm) and S5 (5, 30 and 75 cm) were selected for further investigation by HR-XPS, then samples S2 (65 cm) and S5 (75 cm) were analyzed by SEM–EDS. Eight sediment samples were considered with depth in core S2 (2, 6, 10, 18, 26, 34 and 50 cm) and core S5 (6, 10, 26, 34, 46, 50, 54 cm). The dried out, grinded and sieved samples were then analyzed with XANES spectra in NSRRC in October, 2011.

2.6. Multivariate statistical

Factor analysis (FA) and cluster analysis (CA) are multivariate statistical methods, effective means of manipulating, interpreting and representing data concerning characteristics of water quality and geochemistry (Johnson and Wichern, 1992). Factor analysis is applied to interpret the geochemical characteristics and yields the general relationship between measured chemical variables by elucidating the multivariate patterns that may help to classify the original data. It can be used to determine the geographical distribution of the resulting factors. The geochemical interpretation of factors yields insight into the main processes that may govern the distribution of hydrochemical variables. The first step of factor analysis was to standardize the raw data and make them dimensionless. The correlation coefficient matrix, eigenvalues and eigenvectors were determined to yield the covariance matrix. Then, the data were transformed into factors. Only factors with eigenvalues that exceed one are retained in this work. The contribution of each factor of each porewater samples (factor scores) is computed.

Cluster analysis was used as an analysis of variance approach (hierarchical cluster) to measure a distance between variable clusters, attempting to minimize the sum of squares of any two clusters that could be formed at each step (square Euclidean distance). Hydrogeochemical data with similar properties were clustered in a group. To avoid misclassifications arising from the different order of magnitude of the variables, the variances for each variable were standardized. The Ward's method was used to carry out CA. The obtained CA results assisted to determine the main hydrogeochemical processes of As enrichment in this proposed wetland. Notably the CA is generally used to interpret the hydrochemical data, that is based on factor score (Kim et al., 2005).

In this study, the 18 chemical parameters of the porewater samples, including pH, EC, DO, Eh, As, As^{3+}, Fe, Fe^{2+}, Cl^-, SO_4^{2-}, HCO_3^-, Mn, Ca^{2+}, Mg^{2+}, Na^+, K^+, NO_3^-, and NH_4^+ were considered to evaluate the characteristics of aqueous phase by factor analysis. The factor scores of factor analysis were applied for the calculation of cluster analysis (Kim et al., 2005). Two multivariate statistical methods, FA and CA were performed using SPSS software (SPSS Inc., 1998). They were applied to delineate the vertical profile of redox zonation. According to the ranges of an interval, the samples for isotopic analyses are different with that of samples for chemical analyses. Hence, the six parameters associated with isotopic compositions (Table 2), including $\delta^{34}S_{[SO4]}$, $\delta^{18}O_{[SO4]}$, SO_4^{2-}, FeS_2, $\delta^{34}S_{[FeS_2]}$ and fractionation factor ε ($\varepsilon = \delta^{34}S_{[FeS_2]} - \delta^{34}S_{[SO4]}$), were applied alone for the calculation of FA and CA.

Table 1
Statistical geochemical data of porewater and sediment of redox zonation in Guandu wetland.

Porewater																	Sediment					
Zone[a]		pH	EC (mS/cm)	DO (mg/L)	Eh (mV)	As (μg/L)	As^{3+} (μg/L)	Fe^{2+} (μg/L)	SO_4^{2-} (mg/L)	HCO_3^- (mg/L)	SO_4/Cl	TOC (mg/L)	Fe (mg/L)	Mn (mg/L)	NO_3–N (mg/L)	NH_4–N (mg/L)	TOC (mg/kg)	SO_4^{2-} (mg/kg)	As (mg/kg)	Fe (mg/kg)	Mn (mg/kg)	FeS_2 (mg/kg)
S2 Zone 1	Min	6.8	14.7	7.2	−22.1	0.6	0.0	0.0	704.0	191.1	0.2	8.0	0.2	0.1	0.5	0.1	15.9	1210.0	16.1	37700.0	388.0	0.6
	Max	7.4	15.4	7.7	12.4	6.3	2.1	5.6	895.5	303.5	0.2	26.0	2.2	0.9	1.3	0.2	17.1	1800.0	23.8	43500.0	485.0	0.9
	Mean	7.0	15.1	7.4	0.2	2.7	0.7	1.9	786.3	230.2	0.2	16.7	0.9	0.3	0.8	0.1	16.7	1436.7	19.9	40166.7	437.3	0.7
S2 Zone 2	Min	7.0	16.3	3.7	−48.8	9.9	2.6	5.2	655.2	177.1	0.1	10.0	5.2	1.5	0.3	0.9	13.9	1860.0	11.1	24600.0	223.0	0.4
	Max	7.9	17.7	5.0	1.4	184.7	125.4	22.2	863.2	621.4	0.2	30.0	14.8	2.6	2.4	2.5	23.2	2470.0	17.0	39800.0	313.0	1.8
	Mean	7.3	17.0	4.3	−17.9	43.0	30.4	10.8	790.2	286.0	0.1	17.1	9.2	1.9	1.2	1.6	18.2	2231.4	14.1	32871.4	276.1	1.0
S2 Zone 3	Min	8.0	18.5	2.4	−67.9	6.3	6.3	0.8	884.7	555.8	0.1	6.0	1.8	1.2	0.6	1.4	27.1	2140.0	16.2	26100.0	255.0	1.9
	Max	8.2	20.0	4.7	−57.3	56.3	53.7	3.6	1108.9	641.8	0.2	16.0	6.2	1.7	2.4	2.9	35.4	2850.0	21.2	34700.0	414.0	5.0
	Mean	8.1	19.3	3.5	−63.3	20.6	17.6	2.0	1001.8	599.9	0.1	11.5	3.2	1.3	1.2	2.0	32.8	2584.0	19.7	29720.0	324.8	3.9
S5 Zone 1	Min	6.8	14.2	3.6	−21.7	0.3	0.0	0.0	692.0	172.0	0.1	6.0	0.2	0.2	1.1	0.3	14.1	1380.0	13.1	25600.0	304.0	0.4
	Max	7.4	16.6	6.9	−6.3	7.1	5.6	6.3	892.0	311.2	0.2	10.0	15.2	3.2	2.9	1.8	20.0	2710.0	21.6	41500.0	380.0	2.6
	Mean	7.2	15.8	5.3	−14.6	3.7	3.4	3.9	772.5	252.9	0.2	8.0	6.8	2.1	2.0	0.9	18.0	1993.3	17.5	33140.0	338.0	1.1
S5 Zone 2	Min	7.2	15.6	3.4	−24.3	3.0	1.5	0.2	718.2	264.7	0.1	4.0	1.7	1.8	0.6	1.7	15.9	1720.0	9.5	30400.0	281.0	2.9
	Max	7.5	16.8	3.7	−12.5	10.4	9.7	5.7	800.0	407.9	0.2	10.0	10.9	2.5	2.6	6.5	21.5	2140.0	18.4	41800.0	337.0	10.1
	Mean	7.3	16.1	3.5	−18.8	5.4	4.1	2.3	743.3	318.5	0.1	7.1	7.4	2.1	1.6	3.4	17.0	1891.4	13.7	38228.6	306.7	6.2
S5 Zone 3	Min	7.7	18.4	1.6	−66.0	4.2	7.0	0.0	512.0	492.5	0.1	4.0	3.7	2.3	2.5	8.2	23.1	2300.0	15.8	40800.0	285.0	9.8
	Max	8.1	20.0	4.0	−40.0	23.2	26.4	2.1	572.4	747.3	0.1	12.0	8.7	2.7	2.5	11.0	35.7	2560.0	23.2	42400.0	347.0	12.3
	Mean	7.9	19.4	2.8	−54.4	11.6	13.2	0.6	542.4	625.3	0.1	7.3	5.5	2.5	2.5	9.5	29.1	2430.0	19.1	41600.0	300.8	11.1

[a] Zone 1, Zone 2 and Zone 3 are oxidizing zone, transitional zone and reducing zone, respectively.

3. Results and discussions

3.1. Vertical profiles of hydrochemical characteristics

The tidal effect resulted in high EC values in the outer estuary point (S5) and low EC values in the inner point (S2). The infiltration of rain and surface water diluted the EC values of the porewater in the shallow layer, but had a smaller effect on the deep layer. FA and CA were used to assess the geochemical characteristics of the porewater samples in various depths. Absolute factor loadings higher than 0.7 were included in the factor model. Three factors and four factors were extracted from the 18 chemical parameters by FA in S2 and S5, respectively. Factor 1, salinization, was the most significant factor and had high loadings of Cl^-, EC, K^+, Mg^{2+}, Na^+, Ca^{2+}, pH, EC, HCO_3^- and SO_4^{2-}, the major components of seawater. Factor 1 of S2 constituted 56.3% of the total variances, and S5 accounted for 44.9% of the total variances. The chief geochemical characteristics of S2 and S5 were related to saline water. The source of the saline water in the porewater was the tidal fluctuation of seawater. However, no clear relationship between EC and As concentration was found in two core samples suggesting that salination only had minor effect on the on As mobility in the wetland system. Fig. 2 shows the dendrograms of CA. Based on the factor scores of FA, CA classified all porewater samples into three groups of core S2. Table 1 shows the classified porewater samples of Groups 1, 2, and 3 in the shallow layer (S2-1 to S2-3 and S5-1 to S5-6), middle layer (S2-4 to S2-10 and S5-7 to S5-13), and deep layer (S2-11 to S2-15 and S5-14 to S5-17), respectively.

The vertical variations of the Eh value were measured in all of the porewaters of S2 and S5. Porewater Ehs decreased from the surface zone to the deep zone, (Fig. 3a and b), resembling aqueous As^{3+} and Fe^{2+}, which were dominant species in the core S2 and S5 (Fig. 3c and d). The low levels of aqueous As^{3+} and Fe^{2+} in the core S5 were caused by the dilution from tidal seawater (Table 1). High-aqueous As^{3+} concentrations were found in the middle layer (up to 125.4 μg/L) of S2, and up to 26.4 μg/L in the deep layer of S5, accompanied by decreased Eh values. For the porewater, the oxidation parameters (e.g., DO and Eh values) decreased with depth and the amount of reductive species (e.g., NH_4–N, As^{3+}, Fe^{2+}) that were found in middle and/or deep layers. The vertical redox distributions of S2 and S5 based on depth can be classified as oxidizing, transitional, and reducing zones, respectively.

3.2. Redox zonation

The redox processes were related to the biogeochemical processes of organic compounds in the sediments of the wetland. The vertical distribution of the oxidizing zone was correlated with surface infiltration, where oxygenated river water, seawater, and rainwater with high DO permeated the porewater. The permeated oxidative species (e.g., DO, NO_3^-—N, and SO_4^{2-}) in the porewater, then they may be transported from the oxidizing zone to the reducing zone, except for metal oxides, which originate from sediment. These species act as electron acceptors and can be gradually consumed through the microbial metabolite reactions of organic compounds and reducing matter. Therefore, there was a high concentration of reducing species (e.g. Fe^{2+}, NH_4^+-N, As^{3+}, and Fe^{2+}) in deeper depths. Moreover, according to our previous study, the uptake and bioaccumulation of As in Kandelia obovata were significant. Kandelia obovata acts as an As accumulator in Guandu wetland (Chen et al., 2012). Thus aqueous As concentrations in the oxidizing zone were significantly lower than that in the reducing zone due to the uptake of aqueous As by the mangrove (Table 1).

Aqueous Fe^{2+} concentrations in the porewater of S2 and S5 ranged from 0.01 to 22.2 mg/L and from 0 to 6.3 mg/L, respectively. High aqueous Fe^{2+} concentrations were found in the transitional zone of S2 and in the reducing zone of S5 (Table 1). Fig. 3a and b show the decreased Eh values from the oxidizing zone to the reducing zone and the pH changes from acidic to alkaline conditions, respectively. The occurrence of elevated As in porewater is associated with reducing conditions and correlated with HCO_3^- and Fe (Fig. 3c and d). Liu et al. (2003) suggested that As pollution in groundwater is affected by high aqueous alkalinity and TOC in Southwestern Taiwan. The redox conditions control the dissolution and precipitation of As-bearing minerals and release As to the groundwater. The mineralization of OM progressively promotes the dissolution of calcite, increases alkalinity, and causes the reduction of arsenate to arsenite (Masscheleyn et al., 1991; Nickson et al., 2000). Aqueous As^{3+} was a dominant species in the transitional and reducing zones in both the core S2 and S5 (Table 1). The vertical variation of HCO_3^- in the porewater was correlated with the aqueous As concentration, whereas the reducing potential increased with depth (Fig. 3c and d). In suboxic to anoxic conditions, the presence of dissolved Fe typically corresponds to dissolved As, NH_4^+—N, and HCO_3^-, which is consistent with the

Table 2
Sulfur and oxygen isotopic compositions, ^{34}S enrichment factors, FeS_2 and SO_4^{2-} concentration in shallow and deep samples in core S2 and S5.

No.	Shallow/deep	Zone [b]	Depth (cm)	$\delta^{18}O_{[SO4]}$ (‰)	$\delta^{34}S_{[SO4]}$ (‰)	$\delta^{34}S_{[FeS2]}$ (‰)	FeS_2 (mg/g)	SO_4^{2-} (mg/L)	$\varepsilon^{34}S_{[FeS2-SO4]}$ [a]
S2-a	Shallow	1	5	10.0	20.4	−7.7	0.50	827.4	−28.2
S2-b	Shallow	1	15	11.5	22.6	−11.3	0.82	679.6	−33.9
S2-c	Shallow	2	25	12.0	23.9	−14.4	2.33	827.6	−38.4
S2-d	Shallow	2	35	14.5	27.3	−9.4	2.52	796.1	−36.8
S2-e	Deep	2	45	17.8	41.3	0.3	4.09	814.4	−40.9
S2-f	Deep	3	55	18.3	49.5	2.0	6.67	1098.5	−47.5
S2-g	Deep	3	65	19.5	57.1	2.2	6.76	905.0	−54.8
S2-h	Deep	3	75	18.2	57.6	0.3	4.52	925.4	−57.3
S5-a	Shallow	1	5	9.2	19.0	−7.9	0.92	846.2	−26.9
S5-b	Shallow	1	15	9.8	20.1	−6.3	0.54	741.3	−26.3
S5-c	Shallow	1	25	14.6	24.5	−5.3	1.01	730.0	−29.8
S5-d	Shallow	2	35	15.2	24.5	−6.1	1.03	726.7	−30.6
S5-e	Shallow	2	45	13.8	24.8	−7.5	3.00	732.4	−32.3
S5-f	Deep	2	55	14.8	24.8	−11.0	1.89	783.5	−35.8
S5-g	Deep	2	65	13.7	27.5	−14.1	1.93	630.5	−41.6
S5-h	Deep	3	75	18.6	37.3	−17.1	5.08	542.2	−54.4
S5-i	Deep	3	85	18.1	48.4	−0.3	7.65	572.4	−48.7

[a] The enrichment factor of $\varepsilon^{34}S_{[FeS2-SO4]}$ as $\delta^{34}S$ of pyrite minus $\delta^{34}S$ of sulfate.
[b] Zone 1, Zone 2 and Zone 3 are oxidizing zone, transitional zone and reducing zone, respectively.

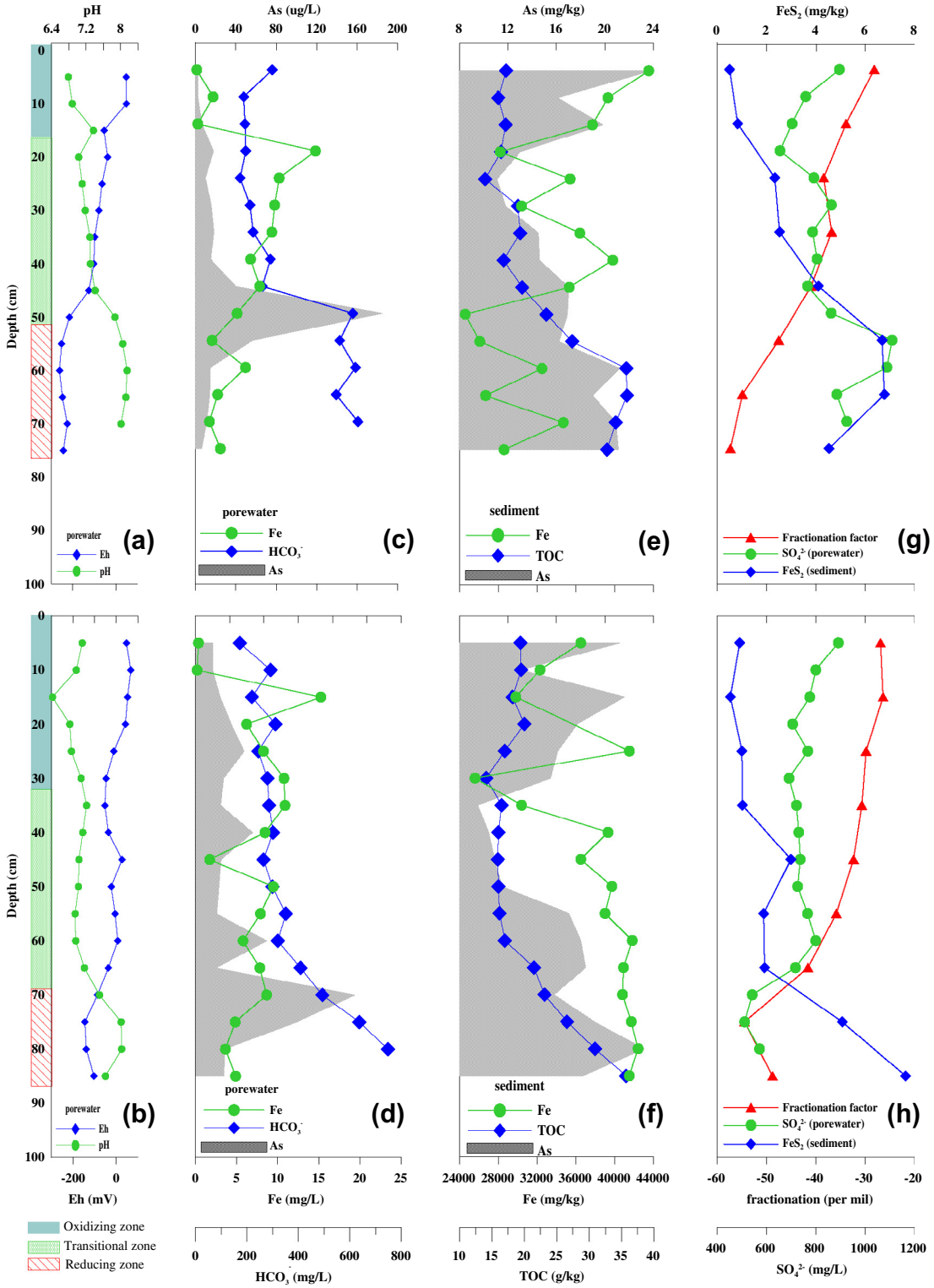

Fig. 3. Geochemical parameters of porewater and solid phase profile of S2 and S5 in the Guandu wetland. Aqueous sulfate, solid FeS_2 and fractionation factor (ε) profiles of S2 and S5 plotted in (g) and (h).

mechanism of the reductive dissolution of Fe-oxyhydroxides through the respiration of OM (Nickson et al., 2000). Appelo et al. (2002) indicated that As can be mobilized by displacement from the sediment surface by contact with highly dissolved bicarbonate water. The enrichment profile of As is similar to that of HCO_3^- in porewater, especially in the interface of transitional and reducing zones (Fig. 3c and d).

Therefore, the mineralization of OM in sediment causes the onset of reducing conditions (Stumm and Morgan, 1996), resulting in the dissolution of As-rich FeOOH and the reduction of adsorbed arsenate to arsenite. In addition, As is released from the solid phase to aqueous phase. The decrease of solid Fe contents with depth (Table 1; Fig. 3e and f) suggests that the reductive dissolution of Fe (hydr)oxides in the transitional zone is likely to occur when the

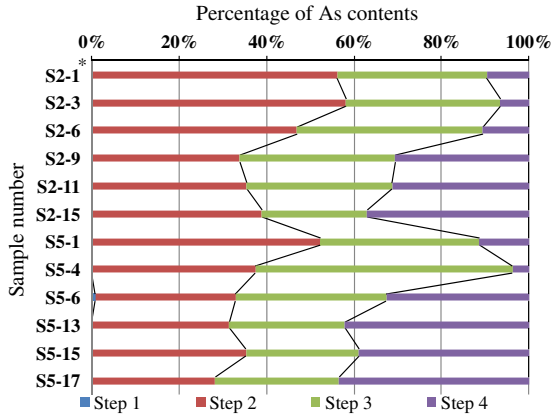

Fig. 4. Arsenic contents as fraction in different extracts of core S2 with depths and core S5 with depths. Steps 1–4 denote exchangeable phase, amorphous metal oxide and carbonate phase, crystalline metal oxides phase, and aluminosilicates and sulfides phase, respectively. *S2-1 the first two alphammerical number denotes the core sample S2 amd third number denotes the depth interval, one interval is 5 cm.

OM contents increase. These processes occurred substantially in S2.

The solid-phase TOC was high in the reducing zone and was correlated with the enrichment of the solid phase As. Under reducing conditions, solid-phase TOC triggers the formation of As-sequestering sulfides, leading to a reduction in As mobility (Xia et al., 1998; Langner et al., 2012). Fig. 3g and h show the increase of solid-phase FeS_2 over depth in both cores. The enrichment of FeS_2 in the reducing zone may cause an As sequestration mechanism in anaerobic natural OM (NOM; e.g., TOC). Trends of increasing solid As concentrations with increasing FeS_2 and TOC were observed (Fig. 3g and h).

3.3. Mineralogical and geochemical characterization of the core samples

Fig. 4 shows the analytical results of the As concentrations in various extracts. However, approximately 60–90% of the extracted As contents were incorporated in the amorphous and crystalline metal oxides (Steps 2 and 3), and the sulfate reduction simultaneously reduced the As mobility. In the oxidizing zone, the aqueous As concentrations with high proportions of Step 2 (58.2% and 52.0% for cores S2-3 and S5-1, respectively) were higher than those in the transitional and reducing zones. The poor concentration of aqueous As in the oxidizing zone may have been caused by the adsorption of aqueous As having increased on the amorphous Fe (hydr)oxides (McArthur et al., 2001; Nickson et al., 2000). The XPS results on the chemical states of the Fe minerals in both core samples over all depths indicated that FeO, FeOOH and Fe_2O_3 were the primary Fe minerals. These results suggest that the As that was adsorbed on the Fe hydroxides in the oxidizing zone was dependent on the enrichment of the solid As and Fe contents (Table 1).

The reduction of As in the amorphous phase (Step 2, including carbon phase) and the increase of the aqueous As concentration in both core samples were found in the boundary between the transitional and reducing zones. The high aqueous As concentration may have been caused by the dissolution of As-rich Fe (hydr)oxides, whereas the NOM was provided during the bacterial respiration and served as the electron donors (Islam et al., 2004; Hossain et al., 2012). The chief As content in the reducing zone was an increase of the sulfides phase (Step 4, Fig. 4); thus, the formation of As-bearing sulfides may be a possible process for immobilizing solid As.

Fig. 5 shows images of the 2 core samples S2-12 and S5-15 obtained using SEM (Fig. 5a and b). The peaks of the spectrogram denote the appearance of Fe, S, Si and O, including As, in the solid sample (Fig. 5c and d). The presence of framboidal diagenetic in

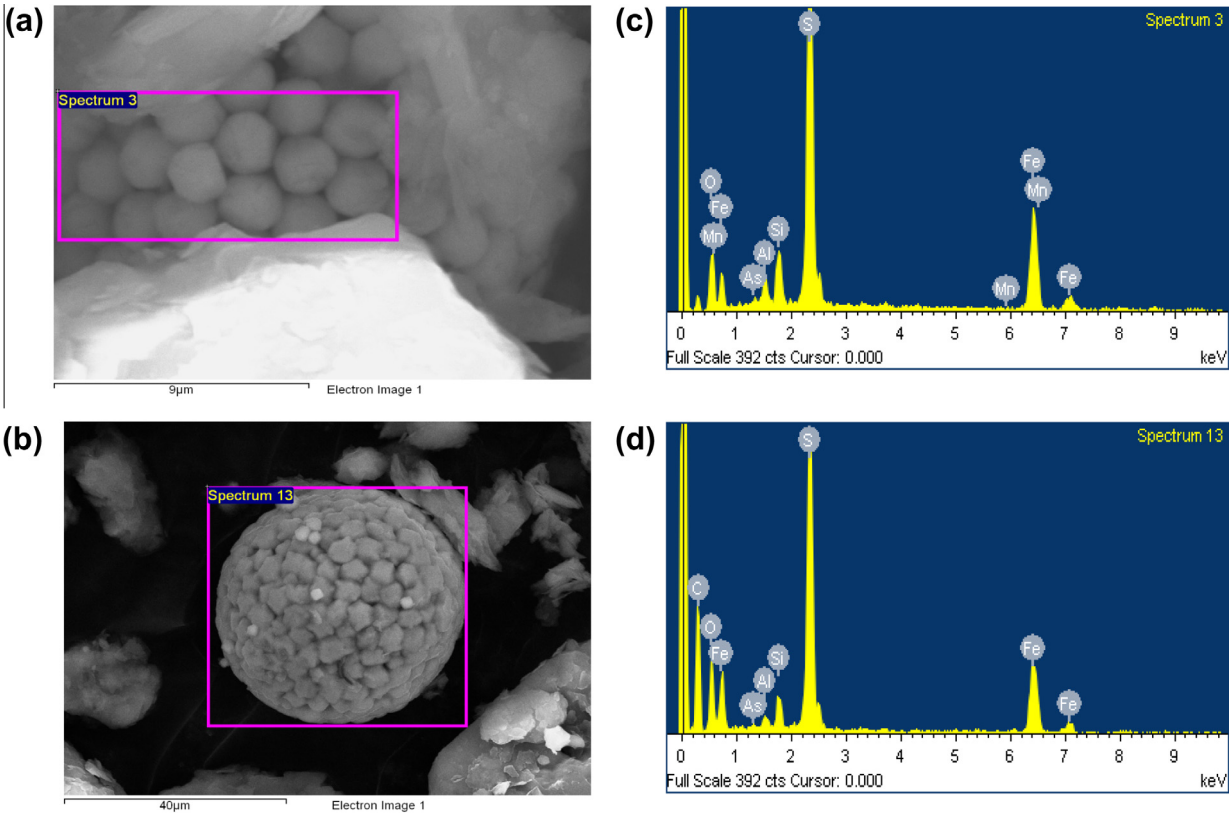

Fig. 5. SEM–EDS analysis of core samples of S2-12 (a) and S5-15 (b); the spectrum of core samples of S2-12 (c) and S2-15 (d).

the reducing zone shows that As may be co-precipitated with pyrite, thereby enriching solid As and FeS_2 concentrations (Table 1).

Fig. 6 shows that the main form of As was As^{5+} (11874 eV) in both core samples analyzed according to the positions and shapes of the absorption edge in the XANES spectra. The deviation of As were obtained for all soil samples corresponding to the As^{5+} standard sample (Fig. 6a and c). Because of the other ions/compounds in the soil sample, the peak of the soil samples exceeds that of the As^{5+} standards. The results obtained suggest that changes in atmospheric oxygen affect the shallow-layer sediment and are easier because of the ebb-tidal influence. The redox variations of core sediment according to depth are primarily governed by intermittent seawater tides. Thus, approximately 62–92% and 60–90% of extracted As concentrations are incorporated in amorphous and crystalline metal oxides, respectively (Fig. 4). According to XPS, despite the occurrence of As-bearing minerals, a major association exists between arsenic and Fe-oxide phases in the solid profile. Hence, the high solid As concentration in the oxidizing zone may be caused by the precipitation of As-bearing Fe oxides and/or complexation with surfaces containing Fe oxides (Waychunas et al., 1993; Farquhar et al., 2002; Sherman and Randall, 2003). Cancès et al. (2005) contended that mainly arsenate (comprising 80%) is associated with the amorphous Fe^{3+} oxides as co-precipitates within the soil profile in slightly acidic and oxidizing conditions. Therefore, our results support those reported by several previous laboratory and field studies (Pierce and Moore, 1982; Yang et al., 2002; Cancès et al., 2005).

Although the As^{5+} is a dominate species, a significant mixture of As^{5+} and As^{3+} occurred from middle to deep depths in both the core S2 and S5 sediment samples (S2: 26–50 cm; S5: 10–54 cm) (Fig. 6b and d). The mixture of As^{5+} and As^{3+} indicates the tendency of As^{5+} to transfer lightly to As^{3+} (Kocar et al., 2008). The maximal concentrations of solid-phase As occurred in the oxidizing zone and reducing zone in both the core S2 and S5, whereas the minimum concentrations of solid-phase As occurred in the transitional zone (Table 1; Fig. 3e and f). The mobility of As in the transitional zone may be caused by the reductive dissolution of the As content in Fe oxides, which depends on the reduction of As^{5+} into As^{3+} when shifting from oxidizing to reducing conditions (Mitsunobu et al., 2006). Under iron-reducing conditions, the dominant As and Fe species were arsenite and ferrous Fe in porewater (Du Laing et al., 2009), which generated As mobility from the solid to the

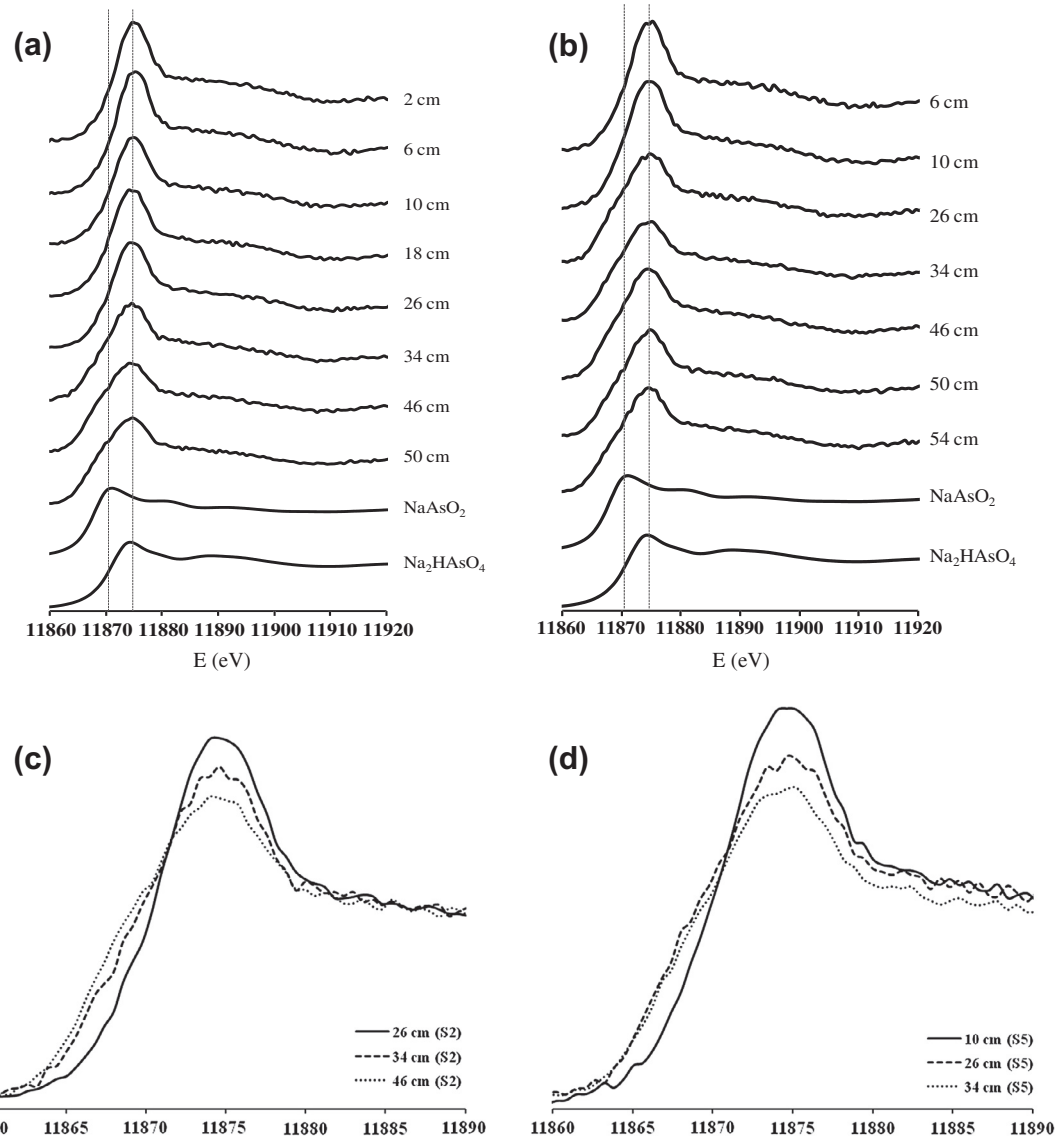

Fig. 6. Arsenic *K*-edge XANES spectra data of selected core samples and reference As standard ($NaAsO_2$ and Na_2HAsO_4) at S2 (a) and S5 (c). The extension of As K-edge XANES spectra data in transitional zones at S2 (b) and S5 (d).

aqueous phase. Arsenite has been found to possess consistently more mobility than As^{5+} in solid phases (Masscheleyn et al., 1991). Moreover, the adsorption ability of As^{5+} is stronger than that of As^{3+} (Laing et al., 2009), thus the sorption distribution coefficient of As^{5+} is much higher than that of As^{3+} (Hu et al., 2012). The mobility of As from sediment to porewater can be attributed to the redox transformation of As species from As^{5+} to As^{3+} (Fig. 6). According to the results of As sequential extraction, XPS and XANES, which are the mobility and bioavailability of solid As, were strongly controlled by NOM. This may trigger the reductive dissolution of As-rich Fe oxides in the transitional zone (Wang and Mulligan, 2006).

The occurrence of FeS_2 content increased with depth (Fig. 3g and h), and framboidal diagenetics (such as pyrite) were identified in the reducing zone using SEM analysis. We observed a general trend of solid As and solid FeS_2 content increasing in the reducing zone (Fig. 3e–h). A significant mixture of As^{5+} and As^{3+} also occurred in the reducing zone, leading to the formation of various surface complexes and poor crystalline arsenic sulfide. Bostick and Fendorf (2003) suggested that As^{3+} can be adsorbed onto Fe sulfide (FeS) and pyrite (FeS_2). Wolthers et al. (2005) reported that both As^{3+} and As^{5+} formed on the surfaces of disordered mackinawite (FeS). Thus, the occurrence of high solid As in the boundary of the transitional and reducing zones can be attributed to the mechanisms of As sorption onto sulfide surfaces (Xia et al., 1998; Wang and Mulligan, 2008; Langner et al., 2012).

3.4. Sulfur cycling and sulfur isotopes

According to the results of FA and CA, all samples in both core S2 and S5 were classified into two groups characterized by shallow layers (S2-a to S2-d and S5-a to S5-e) and deep layers (S2-a to S2-e and S5-f to S5-i), respectively (Table 2; Fig. 7). The $\delta^{34}S_{[SO4]}$ and $\delta^{18}O_{[SO4]}$ isotope compositions of porewater samples ranged between 19.0‰ and 27.3‰ for $\delta^{34}S_{[SO4]}$ and 9.0‰ and 15.2‰ for $\delta^{18}O_{[SO4]}$ in shallow samples, and from 41.3‰ to 57.6‰ for $\delta^{34}S_{[SO4]}$ and 17.8‰ to 19.5‰ for $\delta^{18}O_{[SO4]}$ in deep samples, indicating that differing sulfate sulfide cycling is involved in both S2 and S5. The enrichment of $\delta^{34}S_{[SO4]}$ and $\delta^{18}O_{[SO4]}$ ($\delta^{34}S_{[SO4]} > 27‰$; $\delta^{18}O_{[SO4]} > 13‰$) is in deep samples associated with increases in the Eh value and FeS_2 concentration (Table 1 and 2). The aqueous sulfate in shallow samples of both S2 and S5 is probably formed by the mixing of modern seawater. By contrast, the relative enrichment of $\delta^{34}S_{[SO4]}$ and $\delta^{18}O_{[SO4]}$ in deep samples (e.g., the transitional zone and reducing zone) of both cores is probably caused by (1) the dissolution of ^{34}S- and ^{18}O-enriched sulfate minerals (Taylor and Wheeler, 1994), and (2) the bacterial reduction of sulfate (Fritz et al., 1989; Riedinger et al., 2010). However, the results of SEM and XPS for both cores indicated the absence of sulfate minerals in the study area (Fig. 5). Hence, the dissolution of ^{34}S- and ^{18}O-enriched sulfate minerals is not the only process responsible for the ^{34}S- and ^{18}O-enrichment of sulfate in porewater (Taylor and Wheeler, 1994).

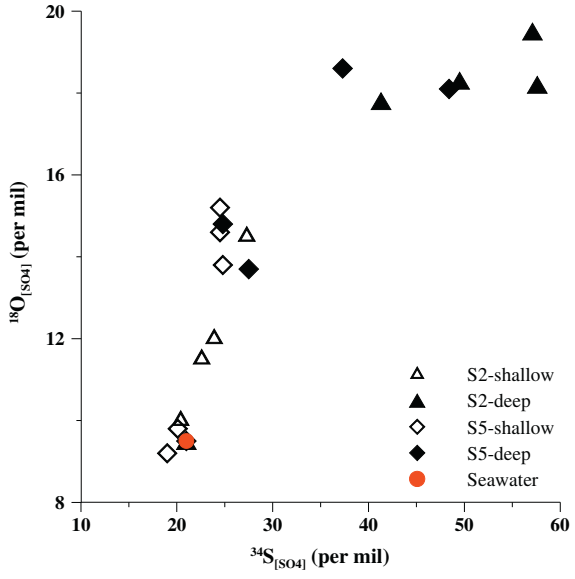

Fig. 7. Scatter plot of $\delta^{18}O_{[SO4]}$ and $\delta^{34}S_{[SO4]}$ in two type porewater samples of S2 and S5. The reference values from seawater are modified from Clark and Fritz (1997).

Sulfate-reducing bacteria (SRB) preferentially extracts sulfate ^{16}O and ^{32}S causing the residual sulfate reservoir to be enriched in with ^{18}O and ^{34}S (Andersson et al., 1992; Böttcher et al., 1998; Zheng et al., 2004). The reduction of SO_4^{2-} is catalyzed by bacteria of the genus Desulfovibrio and others (e.g. Jørgensen, 1982), producing dissolved sulfide mineralized carbon according to the following generalized reactions (Ku et al., 1999):

$$2CH_2O + SO_4^{2-} \rightarrow 2HCO_3^- + H_2S \quad (1)$$

$$2H_2S + 2Fe^{2+} \rightarrow 2FeS + 4H^+ \quad (2)$$

$$FeS + H_2S \rightarrow FeS_2 \quad (3)$$

In Eq. (1), an ongoing SO_4^{2-} reduction can be recognized in the presence of sulfide, slightly reducing the aqueous TOC and SO_4^{2-} concentrations and/or increasing the aqueous HCO_3^- in transitional and reducing zones (Table 1). The main part of the H_2S produced reacts with dissolved Fe^{2+} or Fe^{3+}-oxyhydroxides to form Fe-sulfide minerals (Eqs. (2) and (3)) (Böttcher et al., 2001). After the initiation in Eq. (1), these processes are associated with the relative enrichments of $\delta^{34}S_{[SO4]}$ and $\delta^{18}O_{[SO4]}$ through the dissimilatory sulfate reduction, which results in the occurrence of pyrite (FeS_2) in the reducing zone, as detected by SEM analysis (Fig. 5). After the dissimilatory sulfate reduction, the adsorption of As on the pyrite surfaces that occurs in the reducing environment causes a decline in the sulfur isotopic fractionations factor ($\varepsilon^{34}S_{[FeS2-SO4]} < -40‰$) and an increase of FeS_2 and solid As concentrations at depth (Fig. 3). The dissimilatory sulfate reduction and bacterial disproportionation generated a low $\varepsilon^{34}S_{[FeS2-SO4]}$ value ($<-45‰$) and $\varepsilon_{[SO4-H2O]}$ ($\geqq 8$–10‰) in the reducing environment, respectively (Canfield and Thamdrup, 1994; Habicht and Canfield, 2001; Lipfert et al., 2007; Riedinger et al., 2010). These studies indicate that anaerobic bacterial disproportionation in the presence of MnO_2, FeOOH, and $FeCO_3$ results in reductive dissolution of manganese and iron oxides. Elemental sulfur produced by the oxidation of sulfide with metal oxides can be metabolized by sulfur-disproportionating bacteria to produce sulfate and sulfide (Eq. (4)):

$$4H_2O + 4S^0 \rightarrow 3H_2S + SO_4^{2-} + 2H^+ \quad (4)$$

Subsequently, the enrichment of hydrogen sulfide and aqueous sulfate may occur. In the reducing condition, hydrogen sulfide and FeS may form FeS_2. The presence of increased FeS_2, aqueous SO_4^{2-}, and As concentrations in the boundary of the transitional and reducing zones of S2 may result from bacterial disproportionating reactions, contrasting the smaller increase of FeS_2 and aqueous SO_4^{2-} in S5. This implies that the reductive dissolution of As-containing Fe oxides is associated with sulfur disproportionation (Fig. 3a and g).

However, the lack of S^0 in the extracted reduced inorganic sulfur (data not shown) suggests that the non-significant bacterial disproportionating reaction is not the primary factor responsible for As mobility in both cores S2 and S5. Thus, aqueous As

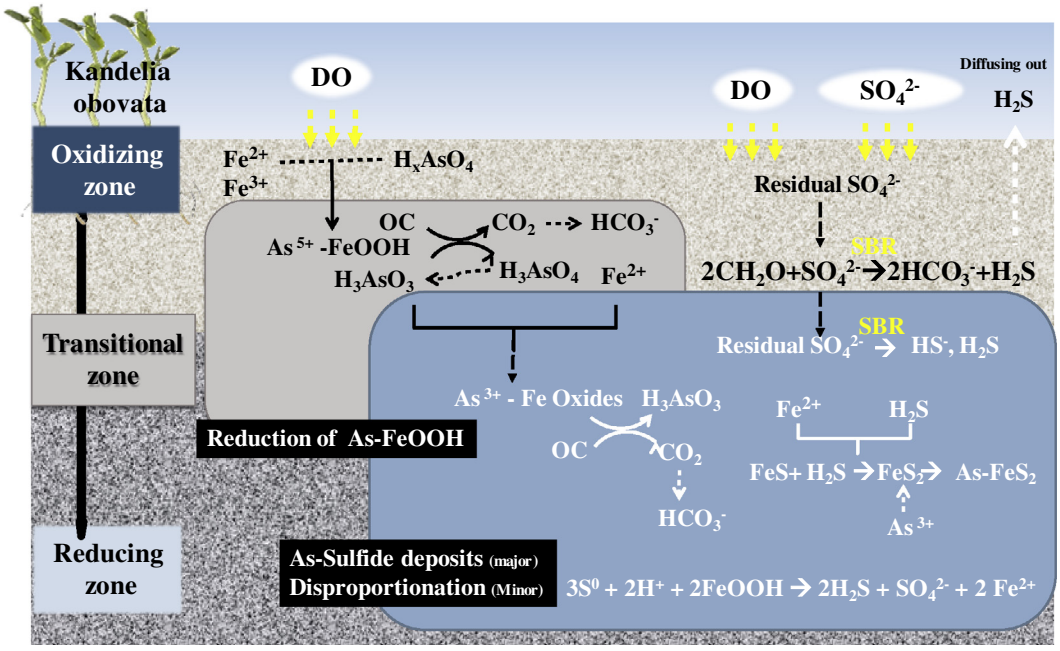

Fig. 8. Conceptual diagram of As redox processes in the Guandu wetland (OC: organic carbon; SRB: sulfate reducing bacteria).

concentrations may be constrained by precipitated sulfide minerals, especially in the reducing zone (Fig. 3c and d). These concentrations result from dissimilatory sulfate reduction and pursuant elevated As and FeS_2 concentrations in sediment (Fig. 3e–h). The probable cause of As mobility in the boundary of the transitional and reducing zones of both cores indicates that the process is governed by the reductive dissolution of Fe oxides combined with the complex cycling of As, Fe, C, and S in wetlands.

3.5. Conceptual model As mobility in the Guandu wetland

This study investigated As mobility in the vertical profiles of the Guandu wetland. The proposed As redox processes in the oxidizing, transitional, and reducing zones are conceptually summarized in Fig. 8. In the oxidizing zone, oxygenated surface water, seawater, and rainwater with high DO permeate into porewater. Under oxic conditions, the Fe oxides provide sufficient adsorption sites for As species (Smedley and Kinniburgh, 2002), leading to low As concentrations in porewater. The redox potential of Fe is equal to or slightly higher than the As in the aqueous phase (Stumm and Morgan, 1996), and combined with reduced Eh values from the oxidizing zone to the reducing zone. The increase of aqueous Fe^{2+} and As^{3+} in the transitional zone indicates that the reductive dissolution of As-containing Fe oxides was catalyzed by the microbially mediated oxidation of NOM (e.g., organic carbon) (Mcarthur et al., 2001, 2004; Mukherjee and Fryar, 2008). Carbonic acid produced during NOM oxidations reacts with sediment to produce high HCO_3^- concentrations that are likely to promote an increase of aqueous As and HCO_3^- in the boundary between the transitional and reducing zones. The minor mobility of As from the sediment to porewater can be attributed to the redox transformation of As species from As^{5+} to As^{3+}, as supported by a petrographic examination of XANES. Some As^{3+} may be re-adsorbed onto the FeOOH in the reducing zone. In the reducing zone, the mineralization of OM progressively drives the reductive dissolution of FeOOH, which results in the co-precipitation of sulfides (Zheng et al., 2004). Aqueous As was constrained by the precipitation of sulfide minerals in the sediment, which resulted from a dissimilatory sulfate reduction and caused an increase in solid As and FeS_2 content. Furthermore, according to the enrichment fractionation factor (ε) of sulfur isotopes, bacterial disproportionation is another probable cause of As mobility, combined with the reductive dissolution of As-containing Fe oxydroxides. Thus, high aqueous As occurred in the boundary between the Fe-reducing and sulfate-reducing conditions of both cores, combined with the mineralization of OM and sulfur disproportionation.

4. Conclusion

Field and laboratory investigations were conducted to explore the As geochemical processes in the Guandu wetland ecosystems of Northern Taiwan. Factor analysis and cluster analysis were employed to characterize the vertical distribution of the porewater geochemistry with redox variation. The redox conditions of porewater in both cores of S2 and S5 could be vertically divided into 3 redox zones, namely the oxidizing, transitional, and reducing zones. In the oxidizing zone, the oxidation products (e.g., DO, NO_3^-—N, and SO_4^{2-}) are primarily controlled by permeated dissolved oxygen. According to the analyses of chemical sequential extraction and XPS, As is readily restrained on the surfaces of amorphous metal oxides, especially FeO, FeOOH, and Fe_2O_3, under oxidation conditions. This results in low aqueous As in the porewater and enriched As and Fe concentrations in the core sediment.

For the transitional zone, moderate reduction conditions facilitate the mobility of As liberated during the reduction dissolution of Fe-oxyhydroxides. A portion of As is re-adsorped/co-precipitated onto the surface of Fe-oxyhydroxide. The analytical results of XANES showed that the significant mixture of As^{5+} and As^{3+} in the sediment occurred in the transitional zone of both cores. This suggests that the alteration redox condition and the transformation of As species are possible mechanisms for As mobility in the transitional zone. In the reducing zone, relative enrichments of $\delta^{34}S_{[SO4]}$ and $\delta^{18}O_{[SO4]}$ values indicate that the significant bacterial sulfate reduction is responsible for the formation of FeS_2, which leads to the immobilization of As^{3+}. The geochemical analysis results of the core sediments showed that the As concentrations increased with elevated FeS_2 and TOC content, indicating that As-bearing pyrite forms during OM respiration. The As release by

the microbial mediated reaction in the salinized aqueous environment is deserved further investigation (Liao et al., 2011)

According to the geochemical analysis results, the As mobility of wetlands is strongly controlled by the oxidation of Fe (hydr)oxides, reductive dissolution of Fe (hydr)oxides, and bacterial sulfate reduction in the oxidizing, transitional, and reducing zones, respectively. Furthermore, high aqueous As is found at the boundaries between the transitional and reducing zones, and accompanied by dissolved Fe and HCO_3^-. Sulfur disproportionation, including the oxidation and reduction of S^0, was also found at deep samples, indicating that As mobility was affected by the redox reactions of sulfate and sulfide. The reductive dissolution of As-containing Fe-oxyhydroxides, redox cycling of sulfate/sulfide, and OM respiration are responsible for the elevated aqueous As concentrations in wetland ecosystems.

Acknowledgements

The authors would like to thank the National Science Council of the Republic of China, Taiwan, for financially supporting this research under Contract No. 98-2313-B-002-053-MY3 and National Taiwan University (NTU), Aim For Top University Project. We are also thankful to National Synchrotron Radiation Research Center (NSRRC), Hsinchu and National Central University, Tao-Yuan, Taiwan, for assisting with the XANES, EDX and SEM studies.

References

Andersson, P., Torssander, P., Ingri, J., 1992. Sulphur isotope ratios in sulphate and oxygen isotopes in water from a small watershed in central Sweden. Hydrobiologia 235–236, 205–217.

APHA (American Public Health Association), 1998. Standard Methods for the Examination of Water and Water Waste, 20th ed. APHA, American Water Works Association, and Water Pollution Control Federation, Washington, DC.

Appelo, C.A.J., Weiden, M.J.V.D., Tournassat, C., Charlet, L., 2002. Surface complexation of ferrous iron and carbonate on ferrihydrite and the mobilization of arsenic. Environ. Sci. Technol. 36, 3096–3103.

Bauer, M., Fulda, B., Blodau, C., 2008. Groundwater derived arsenic in high carbonate wetland soils: sources, sinks, and mobility. Sci. Total Environ. 401, 109–120.

Bostick, B.C., Fendorf, S., 2003. Arsenite adsorption on troilite (FeS) and pyrite (FeS_2). Geochim. Cosmochim. Acta 67, 909–921.

Böttcher, M.E., Oelschlager, B., Hopner, T., Brumsack, H.J., Rullkotter, J., 1998. Sulfate reduction related to the early diagenetic degradation of organic matter and "black spot" formation in tidal sandflats of the German Wadden Sea: stable isotope (^{13}C, ^{34}S, ^{18}O) and other geochemical results. Org. Geochem. 29, 1517–1530.

Böttcher, M.E., Thamdrup, B., Vennemann, T.W., 2001. Oxygen and sulfur isotope fractionation during anaerobic bacterial disproportionation of elemental sulfur. Geochim. Cosmochim. Acta 65, 1601–1609.

Cancès, B., Juillot, F., Morin, G., Laperche, V., Alvarez, L., Proux, O., Hazemann, J.L., Brown Jr., G.E., Calas, G., 2005. XAS evidence of As (V) association with iron oxyhydroxides in a contaminated soil at a former arsenical pesticide processing plant. Environ. Sci. Technol. 39, 9398–9405.

Canfield, D.E., Thamdrup, B., 1994. The production of ^{34}S-depleted sulfide during bacterial disproportionation of elemental sulfur. Science 266, 1973–1975.

Carroll, S.A., O'Day, P.A., Piechowski, M., 1998. Rock–water interactions controlling zinc, cadmium, and lead concentrations in surface waters and sediments, U.S. Tri-State mining district. 2-Geochemical interpretation. Environ. Sci. Technol. 32, 956–965.

Chen, Y.Y., Liu, C.W., Kao, Y.H., 2012. Studies on the Accumulation and Transformation of Arsenic in Ecosystem in Guandu Wetland, Taiwan. EGU General Assembly Geophysical Research Abstracts. Vienna, Austria, 22–27 April 2012, vol. 14, EGU2012-3994, 2012.

Chiang, K.Y., Lin, K.C., Lin, S.C., Chang, T.K., Wang, M.K., 2010. Arsenic and lead (beudantite) contamination of agricultural rice soils in the Guandu Plain of northern Taiwan. J. Hazard. Mater. 181, 1066–1071.

Clark, I., Fritz, P., 1997. Groundwater quality. In: Stein, J., Starkweather, A.W. (Eds.), Environmental Isotopes in Hydrogeology. Lewis, Boca Raton (NY), pp. 142–143.

Dellwig, O., Böttcher, M.E., Lipinski, M., Brumsack, H.J., 2002. Trace metals in Holocene coastal peats and their relation to pyrite formation (NW Germany). Chem. Geol. 182, 423–442.

Du Laing, G., Chapagain, S.K., Dewispelaere, M., Meers, E., Kazama, F., Tack, F.M.G., Rinklebe, J., Verloo, M.G., 2009. Presence and mobility of arsenic in estuarine wetland soils of the Scheldt estuary (Belgium). J. Environ. Monit. 11, 873–881.

Farquhar, M.L., Charnock, J.M., Livens, F.R., Vaughan, D.J., 2002. Mechanisms of arsenic uptake from aqueous solution by interaction with goethite, lepidocrocite, mackinawite, and pyrite: an X-ray absorption spectroscopy study. Environ. Sci. Technol. 36, 1757–1762.

Frau, F., Rossi, A., Ardau, C., Biddau, R., Da Pelo, S., Atzei, D., Licheri, C., Cannas, C., Capitani, C., 2005. Determination of arsenic speciation in complex environmental samples by the combined use of TEM and XPS. Microchim. Acta 151, 189–201.

Fritz, P., Basharmal, G.M., Drimimie, R.J., Ibsen, J., Qureshi, R.M., 1989. Oxygen isotope exchange between sulphate and water during bacterial reduction of sulphate. Chem. Geol. (Isot. Geosci. Sect.) 79, 99–105.

Goldberg, S., 2002. Competitive adsorption of arsenate and arsenite on oxides and clay minerals. Soil Sci. Soc. Am. J. 66, 413–421.

Habicht, K.S., Canfield, D.E., 2001. Isotope fractionation by sulfate-reducing natural populations and the isotopic composition of sulfide in marine sediments. Geology 29, 555–558.

Harvey, C.F., Swartz, C.H., Badruzzaman, A.B.M., Keon-Blute, N., Yu, W., Ali, M.A., Jay, J., Beckie, R., Niedan, V., Brabander, D., Oates, P.M., Ashfaque, K.N., Islam, S., Hemond, H.F., Ahmed, M.F., 2002. Arsenic mobility and groundwater extraction in Bangladesh. Science 298, 1602–1606.

Hossain, M., Williams, P.N., Mestrot, A., Norton, G.J., Deacon, C.M., Meharg, A.A., 2012. Spatial heterogeneity and kinetic regulation of arsenic dynamics in mangrove sediments: the Sundarbans, Bangladesh. Environ. Sci. Technol. 46, 8645–8652.

Hou, X.H., Williams, J., Choy, K.L., 2006. Processing and structural characterization of porous reforming catalytic films. Thin Solid Films 495, 262–265.

Hsieh, Y.P., Shieh, Y.N., 1997. Analysis of reduced inorganic sulfur by diffusion methods: improved apparatus and evaluation for sulfur isotopic studies. Chem. Geol. 137, 255–261.

Hu, Q.H., Sun, G.X., Gao, X.B., Zhu, Y.G., 2012. Conversion, sorption, and transport of arsenic species in geological media. Appl. Geochem. 27, 2197–2203.

Huang, Y.K., Lin, K.H., Chen, H.W., 2003. Arsenic species contents at aquaculture farm and in farmed mouthbreeder (*Oreochromis mossambicus*) in blackfoot disease hyperendemic areas. Food Chem. Toxicol. 41, 1491–1500.

Islam, F.S., Gault, A.G., Boothman, C., Polya, D.A., Charnock, J.M., Chatterjee, D., Lloyd, J.R., 2004. Role of metal-reducing bacteria in arsenic release from Bengal delta sediments. Nature 430, 68–71.

Jessen, S., Larsen, F., Koch, C.B., Arvin, E., 2005. Sorption and desorption of arsenic to ferrihydrite in a sand filter. Environ. Sci. Technol. 39, 8045–8051.

Johnson, R.A., Wichern, D.W., 1992. Applied Multivariate Statistical Analysis, third ed. Prentice-Hall International, Englewood Cliffs, New Jersey, USA.

Jørgensen, B.B., 1982. Mineralization of organic matter in the sea bed-the role of sulphate reduction. Nature 296, 643–645.

Kao, Y.H., Liu, C.W., Wang, S.W., Wang, P.L., Wang, C.H., Maji, S.K., 2011. Biogeochemical cycling of arsenic in coastal salinized aquifers: evidence from sulfur isotope study. Sci. Total Environ. 409, 4818–4830.

Kim, M.J., Nriagu, J., Haack, S., 2000. Carbonate ions and arsenic dissolution by groundwater. Environ. Sci. Technol. 34, 3094–3100.

Kim, J.H., Kim, R.H., Lee, J.H., Cheong, T.J., Yum, B.W., Chang, H.W., 2005. Multivariate statistical analysis to identify the major factors governing groundwater quality in the coastal area of Kimje, South Korea. Hydrol. Process. 19, 1261–1276.

Kocar, B.D., Polizzotto, M.L., Benner, S.G., Ying, S.C., Ung, M., Ouch, K., Samreth, S., Suy, B., Phan, K., Sampson, M., Fendorf, S., 2008. Integrated biogeochemical and hydrologic processes driving arsenic release from shallow sediments to groundwaters of the Mekong delta. Appl. Geochem. 23, 3059–3071.

Ku, T.C.W., Walter, L.M., Coleman, M.L., Blacke, R.E., Martini, A.M., 1999. Coupling between sulfur recycling and syndepositional carbonate dissolution: evidence from oxygen and sulfur isotope composition of pore water sulfate, South Florida Platform, USA. Geochim. Cosmochim. Acta 63, 2529–2546.

La Force, M.J., Hansel, C.M., Fendorf, S., 2000. Arsenic speciation, seasonal transformations, and co-distribution with iron in a mine waste-influenced palustrine emergent wetland. Environ. Sci. Technol. 34, 3937–3943.

Laing, G.D., Chapagain, S.K., Dewispelaere, M., Meers, E., Kazama, F., Tack, F.M.G., Rinklebe, J., Verloo, M.G., 2009. Presence and mobility of arsenic in estuarine wetland soils of the Scheldt estuary (Belgium). J. Environ. Monit. 11, 873–881.

Langner, P., Mikutta, C., Kretzschmar, R., 2012. Arsenic sequestration by organic sulphur in peat. Nat. Geosci. 5, 66–73.

Liao, V.H.-C., Chu, Y.J., Su, Y.C., Hsiao, S.Y., Wei, C.C., Liu, C.W., Liao, C.M., Shen, W.C., Chang, F.J., 2011. Arsenite-oxidizing and arsenate-reducing bacteria associated with arsenic-rich groundwater in Taiwan. J. Contam. Hydrol. 123, 20–29.

Lipfert, G., Sidle, W.C., Reeve, A.S., Ayuso, R.A., Boyce, A.J., 2007. High arsenic concentrations and enriched sulfur and oxygen isotopes in a fractured-bedrock ground-water system. Chem. Geol. 242, 385–399.

Liu, W.C., Hsu, M.H., Kuo, A.Y., Kuo, J.T., 2001. The influence of river discharge on salinity intrusion in the Tanshui estuary, Taiwan. J. Coastal Res. 17, 544–552.

Liu, C.W., Lin, K.H., Kuo, Y.M., 2003. Application of factor analysis in the assessment of groundwater quality in a blackfoot disease area in Taiwan. Sci. Total Environ. 313, 77–89.

Lovley, D.R., Phillips, E.J.P., 1987. Rapid assay for microbially reducible ferric iron in aquatic sediments. Appl. Environ. Microbiol. 153, 1536–1540.

Lytle, C.M., Lytel, F.W., Yang, N., Qian, J.H., Hansen, D., Zayed, A., Terry, N., 1998. Reduction of Cr(VI) to Cr(III) by wetlands plants: potential for in situ heavy metal detoxification. Environ. Sci. Technol. 32, 3087–3093.

Mandal, S.K., Dey, M., Ganguly, D., Sen, S., Jana, T.K., 2009. Biogeochemical controls of arsenic occurrence and mobility in the Indian Sundarban mangrove ecosystem. Mar. Pollut. Bull. 58, 652–657.

Mandal, S.K., Majumder, N., Chowdhury, C., Ganguly, D., Dey, M., Jana, T.K., 2012. Adsorption kinetic control of As(III & V) mobilization and sequestration by Mangrove sediment. Environ. Earth Sci. 65, 2027–2036.
Manning, B.A., Hunt, M.L., Amrhein, C., Yarmoff, J.A., 2002. Arsenic (III) and arsenic (V) reactions with zerovalent iron corrosion products. Environ. Sci. Technol. 36, 5455–5461.
Masscheleyn, P.H., Delaune, R.D., Patrick Jr., W.H., 1991. Arsenic and selenium chemistry as affected by sediment redox potential and pH. J. Environ. Qual. 20, 522–527.
McArthur, J.M., Ravenscroft, P., Safiullah, S., Thirlwall, M.F., 2001. Arsenic in groundwater: testing pollution mechanisms for aquifers in Bangladesh. Water Resour. Res. 37, 109–117.
McArthur, J.M., Banerjee, D.M., Hudson-Edwards, K.A., Mishra, R., Purohit, R., Ravenscroft, P., Cronin, A., Howarth, R.J., Chatterjee, A., Talukder, T., Lowry, D., Houghton, S., Chadha, D.K., 2004. Natural organic matter in sedimentary basins and its relation to arsenic in anoxic ground water: the example of West Bengal and its worldwide implications. Appl. Geochem. 19, 1255–1293.
Mitsunobu, S., Harada, T., Takahashi, Y., 2006. Comparison of antimony behavior with that of arsenic under various soil redox conditions. Environ. Sci. Technol. 40, 7270–7276.
Mukherjee, A., Fryar, A.E., 2008. Deeper groundwater chemistry and geochemical modeling of the arsenic affected western Bengal basin, West Bengal, India. Appl. Geochem. 23, 863–894.
Nickson, R.T., McArthur, J.M., Ravenscroft, P., Burgess, W.G., Ahmed, K.M., 2000. Mechanism of arsenic release to groundwater, Bangladesh and West Bengal. Appl. Geochem. 15, 403–413.
Pierce, M.L., Moore, C.B., 1982. Adsorption of arsenite and arsenate on amorphous iron hydroxide. Water Res. 16, 1247–1253.
Ravel, B., Newville, M.J., 2005. ATHENA, ARTEMIS, HEPHAESTUS: data analysis for X-ray absorption spectroscopy using IFEFFIT. Synchrotron Radiat. 12, 537–541.
Riedinger, N., Brunner, B., Formolo, M.J., Solomon, E., Kasten, S., Strasser, M., Ferdelman, T.G., 2010. Oxidative sulfur cycling in the deep biosphere of the Nankai Trough, Japan. Geology 38, 851–854.
Rothwell, J.J., Taylor, K.G., Ander, E.L., Evans, M.G., Daniels, S.M., Allott, T.E., 2009. Arsenic retention and release in ombrotrophic peatlands. Sci. Total Environ. 407, 1405–1417.
Sherman, D.M., Randall, S.R., 2003. Surface complexation of arsenic(V) to iron(III) (hydr)oxides: structural mechanism from abinito molecular geometries and EXAFS spectroscopy. Geochim. Cosmochim. Acta 67, 4223–4230.
Smedley, P.L., Kinniburgh, D.G., 2002. A review of the source, behaviour and distribution of arsenic in natural waters. Appl. Geochem. 17, 517–568.
SPSS Inc., 1998. SPSS BASE 8.0 – Application Guide. SPSS Inc., Chicago.
Stumm, W., Morgan, J.J., 1996. Aquatic Chemistry: Chemical Equilibria and Rates in Natural Waters. Wiley & Sons, New York.
Taylor, B.E., Wheeler, M.C., 1994. Sulfur- and oxygen-isotope geochemistry of acid mine drainage in the western United States. In: Alpers, C.N., Blowes, D.W. (Eds.), Environmental Geochemistry of Sulfide Oxidation. ACS Symposium Series, vol. 550. Am. Chem. Soc., pp. 414–581.
Wang, I.T., 2005. The Characteristics and the Concentration of Toxic Heavy Metals and Anions of Hot Springs in Taiwan. Master Thesis, National Yang Ming University, Taipei, Taiwan (in Chinese).
Wang, S., Mulligan, C.N., 2006. Natural attenuation processes for remediation of arsenic contaminated soils and groundwater. J. Hazard. Mater. 138, 459–470.
Wang, S., Mulligan, C.N., 2008. Speciation and surface structure of inorganic arsenic in solid phases: a review. Environ. Int. 34, 867–879.
Waychunas, G.A., Rea, B.A., Fuller, C.C., Davis, J.A., 1993. Surface chemistry of ferrihydrite: Part 1. EXAFS studies of the geometry of coprecipitated and adsorbed arsenate. Geochim. Cosmochim. Acta 57, 2251–2269.
Wilkin, R.T., Ford, R.G., 2006. Arsenic solid-phase partitioning in reducing sediments of a contaminated wetland. Chem. Geol. 228, 156–174.
Wolthers, M., Charlet, L., Van der Weijden, H., Van der Linde, P., Rickard, D., 2005. Arsenic mobility in the ambient sulfidic environment: sorption of arsenic(V) and arsenic(III) onto disordered mackinawite. Geochim. Cosmochim. Acta 69, 3482–3492.
Wu, W.C., 2008. Arsenic Distribution in Soil of Rice-paddy and Dry Lands at Guandu Plain. Master Thesis, Department of Soil Environmental Science, National Chung Hsing University (in Chinese).
Xia, K., Weesner, F., Bleam, W.F., Bloom, P.R., Skyllberg, U.L., Helmke, P.A., 1998. XANES studies of oxidation states of sulfur in aquatic and soil humic substances. Soil Sci. Soc. Am. J. 62, 1240–1246.
Yanagisawa, F., Sakai, H., 1983. Preparation of SO_2 for sulphur isotope ratio measurements by the thermal decomposition of $BaSO_4$–V_2O_5–SiO_2 mixtures. Anal. Chem. 55, 985–987.
Yang, J.K., Barnett, M.O., Jardine, P.M., Basta, N.T., Catseel, S.W., 2002. Adsorption, sequestration, and bioaccessibility of As(V) in soils. Environ. Sci. Technol. 36, 4562–4569.
Zheng, Y., Stute, M., van Geen, A., Gavrieli, I., Dhar, R., Simpson, H.J., Schlosser, P., Ahmed, K.M., 2004. Redox control of arsenic mobilization in Bangladesh groundwater. Appl. Geochem. 19, 201–214.